The mechanism and effect of BMP2 mutant L51P in promoting bone formation and osteoblast differentiation induced by BMP2

By

Hany Mohamed Hanafy KHATTAB
DDS, M.Sc.

Thesis

Submitted for partial fulfillment of Doctorate Degree in the Department Oral Rehabilitation and Regenerative Medicine

Supervisor

Professor Takuo KUBOKI

Chairman of the Department of Oral Rehabilitation and Regenerative Medicine,

Dean Okayama University Graduate School of Medicine, Dentistry and Pharmaceutical Sciences

Okayama University, Japan

2014

بسم الله الرحمن الرحيم

“And we have commanded man to be good towards parents; his mother bore him with hardship, and delivered him with hardship; and carrying him and weaning him is for thirty months; until when he reached maturity and became forty years of age, he said, "My Lord! Inspire me to be thankful for the favors you bestowed upon me and my parents, and that I may perform the deeds pleasing to you, and keep merit among my offspring; I have inclined towards you and I am a Muslim”

Introduction

Bone is a dynamic biological tissue composed of metabolically active cells that work in a synchronized manner to maintain a steady remodeling state and to promote healing and efficiently restore of function following fracture [1, 2]. Bone fractures are clinical complications that affect hundreds of thousands of individuals worldwide, [2, 3] and although fracture healing generally present a natural and favorable course, failure rates as high as 5-10 % have been recorded. Such failures are often accompanied by complications resulting in significant patient morbidity, psychological stress and a substantial economic cost to society [4, 5].

As a result of the key discovery and understanding of the molecular osteoinductive agents in bone biology, subsequent production of bone morphogenetic proteins (BMPs) has suggested the possibility of a healing osteoinductive promoter that could be safe and effective in tissue-engineering context [6]. Currently, BMP2 and BMP7 have been approved by the Food and Drug Administration (FDA) for clinical applications. Although encouraging results have been achieved, clinical trials have shown that large doses of BMPs are required to induce successful bone healing in large mammals and humans [7-9]. Such dosages may lead to serious side effects [10].

BMP signaling is initially activated when BMPs bind to the heterotetrameric complexes of type I and type II serine/threonine kinase receptors that are found on the surface of almost all normal cells [11]. Many extracellular proteins capable of down-regulating BMP signaling have been identified [12-14]. Accordingly, the increased expression of BMP antagonists during healing may contribute to the high exogenous concentration of BMPs needed to promote healing [15, 16]. Once the specific binding site of the BMP ligands to their receptors was identified, L51P was produced. L51P is an *in vitro* engineered BMP2 variant with a leucine to proline substitution at codon 51. L51P is deficient in type I receptor binding only. Importantly, L51P binding to the type II receptor and protein molecules such as noggin are unchanged by this amino acid substitution [17, 18]. Although previous studies from our collaborators have shown that L51P enhances the osteoinductive activity of exogenous BMP2 [18, 19], the biological mechanism of L51P in counteracting the BMP antagonists induced by exogenous BMP2 administration remains unclear. It is also unknown whether the targeting time of BMP antagonists would change osteogenic potential of BMP2. For this reason, we hypothesized that the delayed addition of L51P would enhance the ability of BMP2 to

induce bone formation.

In the current study, we investigated whether the simultaneous or delayed addition of L51P to BMP2 promoted the BMP2-induced osteoinduction of MC3T3-E1 and C2C12 cells while accelerating the re-ossification of *in vivo* critical-sized calvarial defects. The molecular mechanism of the effect of the delayed addition of L51P to BMP2 on enhancing BMP2 activity was also investigated

Materials and Methods

Cells, recombinant proteins and culture medium

The osteoblastic cell line MC3T3-E1, previously established from mouse C57BL/6 calvaria, was selected on the basis of its high alkaline phosphatase (ALP) activity in the resting phase, and purchased from Riken Cell Bank, Japan. MC3T3-E1 cells were grown in Dulbecco's Modified Eagle's Medium (Invitrogen, Carlsbad, CA, USA) supplemented with 10 % fetal bovine serum (FBS; Invitrogen), 1 % glutamine, and 1 % antibiotic-antimycotic (Invitrogen) [Basal medium]. Two days after plating, the cells were treated with BMP2 (100 ng/mL) and/or L51P (10 ng/mL and 100 ng/mL). BMP2 and L51P were biologically produced by the Department of Physiological Chemistry, University of Wüzburg, Germany.

Real-time RT-PCR analysis

For the real-time RT-PCR analysis, cells (1×10^5) were seeded in 6-well plates and maintained for 1, 3, or 7 days in culture media. Total cellular RNA was extracted using RNeasy kit (Qiagen, Gaithersburg, MD, USA) according to the manufacturer's protocol. The cDNA was produced by reverse transcription of the RNA using iScript cDNA

Synthesis kit (Bio-Rad, Hercules, CA, USA). Real-time RT-PCR reaction was performed using iQ SYBR Green Supermix (Bio-Rad) and Chromo4^{TM} real-time detector. Primers were designed using Beacon Software (Bio-Rad), with parameters set for use with real-time RT-PCR with a Tm of 62 °C ± 3 °C and an amplicon size of 75 to 200 bp (Table 1). Gene expression levels of the target genes are shown relative to the internal standard mouse ribosomal protein *S29*.

Luciferase reporter assay

To measure the BMP activity, C2C12 cells were stably transfected with a reporter plasmid consisting of the BMP-responsive element (BRE) from the Id1 promoter fused to the luciferase reporter gene (C2C12-BRE-Luc) [20]. These cells were a kind gift from Dr. L Zilberberg and Dr. D Rifkin (New York University School of Medicine, NY, USA).

C2C12 cells were seeded at a density of 4×10^3 cells/well in 96-well white plates and maintained in basal medium. After 24 hours, the cells were stimulated with BMP2 (100 ng/mL) and/or L51P (10 ng/mL, 100 ng/mL). One day after stimulation, the luciferase

activity was measured using Bright-Glo Luciferase Assay System (Promega, Madison, WI, USA) and a microplate luminometer (Glomax 96 Micro Plate Luminometer, Promega), according to the manufacturer's instructions.

Western blot analysis

The stimulated cells were lysed with PhosphoSafe™ Extraction buffer (Merck, Madison, WI, USA). The total protein concentration was determined using Pierce®BCA Protein assay kit (Pierce-Thermo Scientific, Rockford, IL, USA). Ten micrograms of the total protein lysate was electrically separated in a pre-cast polyacrylamide gels (NuPAGE® Novex 4-12 % Bis-Tris Gel, Invitrogen) and transferred electrophoretically to polyvinyl difluoride (PVDF) membranes (GE Healthcare, Buckinghamshire, UK) at 30 V for 2 hours. The membranes were blocked and blotted with antibodies to p-SMAD-1/5/8 (1:1000; Cell Signaling, Danvers, MA, USA), total-SMAD-1 (1:1000; Cell Signaling) and β-ACTIN as a loading control (1:5000; Sigma). Membranes were washed and probed with secondary antibodies and then visualized with ImageQuant LAS 4000 mini (Fujifilm, Tokyo, Japan).

Alizarin red S and ALP staining

MC3T3-E1 cells were seeded on 12-well plates at a density of 4×10^4 cells/well and cultured until they reached confluence. Basal medium containing 100 μM dexamethasone and 2 mM β-glycerophosphate (Sigma, St Louis, MO, USA) was added to induce osteogenic differentiation in the presence or absence of BMP2 (100 ng/mL) and/or L51P (10 ng/mL, 100 ng/mL). For the ALP staining, cells were fixed in 4 % paraformaldehyde (PFA) for 3 min at room temperature (RT), washed with phosphate-buffered saline (PBS) and incubated in the dark for 10 min at RT with a 5-bromo-4-chloro-3-indolyl phosphate/nitroblue tetrazolium (BCIP/NBT) liquid substrate (Roche Diagnostics GmbH, Penzberg, Germany).

After 28 days, calcium deposits were detected by staining with 1 % Alizarin Red S (pH 6.4, Sigma). To quantify the intensity of the stained nodules, dye was solubilized using 0.5 % SDS in 0.5 N HCL for 30 min at RT and measured by reading its optical absorbance at 405 nm.

Cell-protein binding assay

To assess the direct effect of L51P on the cell binding affinity of BMP2, MC3T3-E1 cells were seeded at 1×10^4 in 96-well plates until reaching confluence. Cells were fixed for 20 min at RT with 4 % PFA, washed and pre-blocked in 5 % goat serum (Invitrogen) and 0.05 % BSA (blocking medium) for 20 min at RT. Cells were incubated in 500 ng/mL BMP2 and varying concentrations of L51P for 4 hours at RT in a pre-conditioned medium (0.1 % basal medium collected from cells stimulated with 500 ng/mL BMP2 for 3 days) and then washed carefully with PBS. Groups of fixed cells were incubated with 500 ng/mL BMP2 in 0 % FBS culture medium to determine the effect of the conditioned medium on the cell binding affinity of BMP2. Bound BMP2 ligands were detected by incubating the cells with anti-BMP2 antibody (1:100; Abcam, Cambridge, UK) overnight at 4 ºC. Then, cells were washed and incubated with the corresponding horseradish peroxidase (HRP)-conjugated secondary antibody (1:1000; Santa Cruz Biotechnology, Santa Cruz, CA, USA) for 1 hour at RT. The amount of bound BMP2 was determined by 3,3′,5,5′-tetramethylbenzidine (TMB) colorimetric substrate (Cell Signaling) for 10 min at RT. The reaction was terminated with an equal volume of 2 N

H_2SO_4, and the optical absorbance was measured at 450 nm.

An *in vivo* model of ectopic bone formation

To obtain an *in vivo* controlled release system for BMP2 and L51P, biodegradable hydrogels made from gelatin by glutaraldehyde cross-linking were used and prepared as described in previous reports [21]. To investigate the efficiency of L51P in enhancing BMP2-induced ectopic bone formation, protein-loaded biodegradable hydrogels were subcutaneously implanted in 10-week-old mice for 2 weeks, as reported previously [22]. Briefly, 8 sheets of the biodegradable hydrogel (6 μg and 10 × 10 cm) were soaked in BMP2 (10 μg) and/or L51P (10 μg) with distilled water as a control. Hydrogels were harvested 2 weeks post implantation to assess the level of ectopic ossification. All animals were handled according to the approved protocols and guidelines of the animal committee of Okayama University (OKU-2010433).

An *in vivo* rat model of critical-sized calvarial bone defects

Rats were anaesthetized with isoflurane inhalation, followed by a mixture of xylazine (8 mg/kg; Bayer, Tokyo, Japan) and ketamine (80 mg/kg; Sankyo, Tokyo, Japan) injected intraperitoneally as described previously [23, 24]. The dorsal part of the cranium was shaved aseptically, and a sagittal incision of approximately 20 mm was opened over the scalp of each animal. A 6.5-mm critically sized calvarial defect was subsequently created using a trephine bur under sterile saline irrigation in the center of each parietal bone. Calvarial defects were then implanted with hydrogels preloaded with BMP2 (5 μg) and/or L51P (1 μg, 5 μg). The rats were separated into eight different treatment groups with 3 to 4 rats per group, and the animals were sacrificed after 4 weeks (Table 2).

X-ray and micro-tomographic analyses

Radiographic images were generated with the micro-radiographic apparatus mFX-1000 (Fujifilm, Tokyo, Japan). Micro-computed tomography (micro-CT) images of the calvarial bone were obtained using SkyScan 1174 compact micro-CT (SkyScan, Aartselaar, Belgium). The x-ray source was operated at maximum power of 50 KV and

at 500 μA. Scans were performed at a resolution of 16 μm, after which 269 sections were reconstructed to produce the final calvarial images using SkyScan software (NRecon, CTAn, CTvol and CTVox, SkyScan). ImageJ (ImageJ, JAVA-based free software) was used to assess the level of *bone healing.* The radio-opacity of approximately equal micro-CT images of the newly-formed bone was measured by assessing equal squares around the defects. The mean normalized rate of the radio-opacity was calculated by dividing the mean radio-opacity of the defect by that of the normal bone of a rat of the same age without operation.

Histology and immunohistochemistry

Tissues were fixed in 4 % PFA for 72 hours and decalcified with ethylenediaminetetraacetic acid (EDTA) for 3 weeks. Standard hematoxylin and eosin (HE) staining was performed for histological observation. For osteocalcin (OCN) immunohistochemical (IHC) analysis, paraffin-embedded tissue sections were deparaffinized, blocked in 10 % normal goat serum (Invitrogen) for 30 min at RT, and incubated for 1 hour at RT with anti-OCN antibody (1:150, Takara, Otsu, Japan). Slides

were then washed and incubated with second antibody and 3-amino-9-ethyl carbazole (AEC) color developing reagent (Super Picture^{TM} HRP Polymer Conjugate Broad Spectrum, Invitrogen), according to the manufacturer's instructions.

TRAP staining

Tissues were stained with tartrate-resistant acid phosphate (TRAP) to identify osteoclasts through a 1-hour incubation at 37 ˚C in 10 mg of naphthol AS-BI phosphate, 500 µL of N,N-dimethylformamide, 50 mL of distilled water, 50 mL of 0.2 M acetate buffer (pH 5.0), 60 mg of Fast Red Violet LB salt and 0.75 g of tartaric acid (50 mM) All reagents were purchased from Sigma.

Statistical analysis

The results are expressed as the mean ± SD. Comparisons of two groups were performed using the unpaired Student's *t*-test. Comparisons of three or more groups were performed using a one-way ANOVA; post hoc analyses were performed using Tukey multiple-comparison test. Real-time RT-PCR data of the BMP antagonists were

analyzed by a two-way ANOVA. Differences were considered statistically significant when $p < 0.05$.

Results

L51P enhances BMP2-induced downstream signaling events

To analyze whether L51P has a direct effect on BMP2 signaling cascades, early signaling events downstream of the BMP receptors were investigated by western blot. MC3T3-E1 cells were stimulated with BMP2 (100 ng/mL) and/or L51P (10 ng/mL, 100 ng/mL) for 5, 15, 30, 60, 120, 240 minutes and for 24 and 48 hours. According to previous reports, BMP2, but not L51P, strongly induces SMAD-1/5/8 phosphorylation [18, 19, 25]. Similarly, our data showed a strong activation of p-SMAD at 15 min after stimulation with BMP2 or BMP2/L51P combination (Fig. 1A). On the other hand, treatment with L51P alone did not activate SMAD signaling, but enhanced BMP2-induced SMAD-1/5/8 phosphorylation after 15 min of stimulation (Fig. 1A).

In order to confirm whether activation of SMADs were also associated with activity of BMP2-induced gene reporter, we used C2C12-BRE-Luc cells to analyze Id1 promoter activity. C2C12-BRE-Luc cells were stimulated with BMP2 (100 ng/mL) and/or L51P (10 ng/mL, 100 ng/mL), and after twenty-four hours, luciferase activity was assessed. As shown in Fig. 1B, luciferase activity was significantly enhanced by BMP2 (2.78 fold) and BMP2/L51P combination (4.58 fold) compared to the control group. In

contrast, no significant increase in the Id1 promoter activity could be observed when cells were stimulated with L51P alone, which are in agreement with the results observed with non-activation of p-SMAD by L51P alone (Fig. 1B).

The combination of L51P and BMP2 promotes osteogenic differentiation of MC3T3-E1 cells

We next examined the gene expression levels of early osteogenic markers following stimulation with BMP2 and/or L51P. After 1 day, alkaline phosphatase (*Alp*) and osterix (*Osx*) gene expression levels in BMP2/L51P combination group clearly increased by 1.62 and 1.56 fold respectively, compared to BMP2-treated group. Strikingly, marked and significant differences in the expression levels of the two marker genes - a 3.84-fold increase for *Alp* and 3.74-fold increase for *Osx* - were observed after 3 days, compared to BMP2 group (Fig. 1C, D). Accordingly, a significant difference in Collagen type I (*Col I*) mRNA expression levels was observed between BMP2/L51P combination group and the BMP2 group after 7 days of induction (data not shown). Interestingly, after 3 days of BMP2 treatment, we observed a decrease in the gene expression levels of *Alp*

and *Osx*, which could be due to a feedback response of BMP antagonists. In contrast, the expression levels of the two genes remained nearly constant in the BMP2/L51P combination group, which indicate that the maintenance of *Alp* and *Osx* mRNA at high levels after 3 days of stimulation with BMP2/L51P combination could possibly be correlated with a control of BMP antagonists by L51P.

We then investigated the gene expression levels of main BMP2 antagonists - Noggin, Chordin and Gremlin - during the initial stage of BMP2-induced osteogenesis of MC3T3-E1 cells. Our results showed that *Noggin* (*Nog*), Gremlin 1 (*Grem 1*) and Chordin (*Chord*) gene expression levels were significantly enhanced after addition of 100 ng/mL BMP2 for 24 and 72 hours (Fig. 2A, B, C). Taken together, these results suggest that activation of BMP antagonists after 1 or 3 days corresponds timely, and could be associated with suppression of BMP2-induced increase in the expression levels of *Alp* and *Osx* at day 3 (Fig. 1C, D). Moreover, it is likely that the timing of L51P induction plays an important role in BMP2-induced osteoblast differentiation. Therefore, we next investigated the effect of delayed addition of L51P, after 3 days of BMP2 stimulation, on BMP downstream signaling and osteogenesis of MC3T3-E1 cells.

Delayed addition of L51P strongly enhanced BMP2-induced downstream signaling

To test this hypothesis, we performed western blot analysis for MC3T3-E1 cells after 3 days of BMP2 induction followed by 15 min of L51P stimulation. Under this condition, p-SMAD-1/5/8 was distinctly detected in the delayed L51P/BMP2 combination group compared to BMP2 group (Fig. 3B). To confirm a direct action of the delayed addition of L51P, a luciferase assay was performed. Our results showed that under delayed stimulation of BMP2 by L51P, luciferase activity of Id1 promoter was dramatically enhanced by 2.58-fold compared to BMP2 alone (Fig. 3C). Of note, luciferase activity was enhanced by 1.64-fold under simultaneous BMP2/L51P stimulation compared to the BMP2 group (Fig. 1B). In accordance with the results of western blot and luciferase assay, after the first day of delayed stimulation with L51P, we observed an increase in the *Alp* (1.97-fold) and *Osx* (2.08-fold) expression levels compared to those of the BMP2-stimulated group (Fig. 3D, Table 3). Similarly, delayed stimulation with L51P resulted in a significant increase in both *Alp* and *Osx* gene expression levels after 7 days of osteogenic induction of MC3T3-E1 cells (Fig. 3F). We also used an ALP staining

assay to assess osteogenic differentiation of the delayed L51P application. Interestingly, we found a remarkable increase in ALP staining in the L51P/BMP2 combination group relative to the cells treated with BMP2 alone (Fig. 3E). Taken together, these results present a cell-based perspective on the mechanisms of the potential effect of L51P in modulating the activity of BMP antagonists to enhance BMP signaling for promotion of osteoinduction.

L51P enhances BMP2 cell-binding affinity under BMP antagonist-rich conditions

To determine whether L51P can directly regulate BMP2 cell binding affinity, we performed a cell protein binding assay under conditions rich in BMP antagonists [26]. To enrich the medium with BMP antagonists, MC3T3-E1 cells were cultured in 0.1 % serum medium and stimulated with BMP2 at a concentration of 500 ng/mL. After 3 days, the medium supposedly containing high levels of BMP antagonists was collected and used as the conditioned medium for further experiments. As shown in Figure 4A, a significant decrease in the BMP2-to-cell binding affinity was observed in the cells cultured with conditioned medium, compared to those cultured in normal medium, in

the presence of exogenous BMP2. Our data thus suggest that the conditioned medium is loaded with BMP antagonists that are able to significantly affect the cell binding affinity of BMP2. Therefore, we speculated that L51P may bind to these antagonists and thereby recover the BMP2 binding capacity. In fact, we found that 500 ng/mL L51P increased the cell binding capacity of BMP2, although this increase did not reach significance. However, BMP2 binding affinity was completely restored after stimulation with 1000 ng/mL L51P. Because this experiment provided further evidence for the direct effect of L51P on BMP2 cell binding affinity, we next sought to determine whether the delayed addition of L51P would directly affect the cell binding affinity of the BMP2 in the conditioned medium. To address this question, the cells were incubated in conditioned medium and stimulated with L51P alone. Interestingly, we were able to demonstrate that L51P alone significantly increased the cell binding capacity of the BMP2 ligands in the conditioned medium (Fig. 4B). This effect is especially remarkable because it occurred in the complete absence of exogenous BMP antagonists. In addition, we believe that the most important observation in this experimental model is the increased binding capacity of the BMP2 ligands in conditioned medium after delayed L51P stimulation.

The BMP2/L51P combination promotes the osteogenic differentiation of MC3T3-E1 cells

It remains unclear whether L51P can enhance BMP2-induced osteogenic differentiation under long-term *in vitro* culture conditions. Therefore, MC3T3-E1 cells were stimulated with BMP2 and L51P for 1 and 4 weeks. After 1 week of osteogenic induction, the BMP2/L51P combination group cells stained to some extent more positively for ALP than the BMP2 group cells. By contrast, cells grown in the regular and L51P culture media did not show obvious ALP staining (Fig. 5A). The induced osteogenic phenotype was further confirmed by Alizarin red S staining, which detected extracellular calcium deposition. As shown in Fig. 5A, a higher level of calcium deposition was observed in BMP2/L51P combination group relative to the BMP2 group after 4 weeks of osteogenic induction. However, cells without BMP2 induction stained very weakly for the Alizarin red S staining. In addition, quantitative analysis of the Alizarin red S staining revealed that the MC3T3-E1 cells treated with osteogenic substrate and BMP2/L51P combination significantly produced more mineralized matrix than the BMP2 treated

cells (Fig. 5B). Consistently, Osteocalcin (*Ocn*) expression was significantly enhanced after 3 weeks of BMP2/L51P stimulation (Fig. 5C). Taken together, these data strongly suggest that the osteogenic induction of BMP2 is enhanced when coupled with the addition of L51P.

L51P enhances BMP2-induced ectopic bone formation

To further analyze the interaction between BMP2 and L51P, we induced ectopic bone formation for 2 weeks in a mouse model by subcutaneously implanting protein-loaded biodegradable hydrogels. Using this *in vivo* system, it was possible to investigate the function of L51P on BMP2-induced ectopic bone formation. Our radiographic and histological analyses of the BMP2 and BMP2/L51P-adsorbed hydrogels demonstrated the induction of ectopic bone formation compared to control. Notably, this ectopic bone formation could not be detected in both the L51P and the control groups (Fig. 6E, F, I, J). In terms of the ectopic bone nodule size, BMP2-induced ossicles were present to a lesser degree than in the BMP2/L51P combination group (Fig. 6G, H). HE staining analysis revealed that more bone-like tissue was formed in the BMP2/L51P

combination group (Fig. 6K, L). Furthermore, a trend towards a reduction in bone formation inside the BMP2 group ectopic mass was observed, suggesting the possibility there were differing environmental conditions between the groups (Fig. 6M, O).

L51P enhances BMP2-induced orthotopic bone formation

We further investigated the capability of L51P to induce *in vivo* bone regeneration and repair of critical-sized defects in the rat calvaria. Eight experimental groups were assessed after 4 weeks of healing, as described in Table 2. Radiographs and micro-CT scans were used to assess the resulting bone regeneration. Defects that were left empty or that were treated with only hydrogel showed no healing in the micro-CT scans after 4 weeks. Importantly, groups treated with different concentrations of L51P alone showed no signs of bone healing (Fig. 7A). In contrast, groups treated with the BMP2/L51P combination showed robust healing, which can be observed in the micro-CT images as well as in the quantitative analysis of the percentage of bone healing based on the grey pixels in the defect area. Our results showed an 11 % of healing for the control group, 12 % for the L51P group, and 18 % for the BMP2 group. Importantly, defects treated

with the BMP2/L51P had an impressive healing rate of 48 % (Fig. 7B). To confirm our radiographic findings, histological analysis was performed to evaluate the amount of bone deposition across the defect. Our histological findings identified substantial bone formation in the BMP2/L51P combination groups (Fig. 8G, H), modest bone formation in BMP2 group (Fig. 8F) and no bone formation in the L51P and control defect groups (Fig. 8B-E). Since active bone regeneration occurs through a marked activation of recruited osteoblasts and osteoclasts to the site of regeneration [27]. we performed immunohistochemical analysis for detection of OCN positive mature osteoblasts and TRAP staining for detection of osteoclasts. The results showed a positive OCN staining throughout the healing of BMP2-treated defects, and this staining was more prominent in the BMP2/L51P combination group (Fig. 9A-D). Additionally, an increased intensity of TRAP staining was noted in the defect site treated with BMP2/L51P compared that treated with BMP2 alone (Fig. 9E-H). Taken together, these data confirm that L51P plays an important role in enhancing BMP2-induced bone formation.

Discussion

This study contributes to the current understanding of the function of L51P as a novel up-regulator of BMP osteogenic potential. We demonstrated that L51P influences the osteoinduction efficiency of BMP2. This was demonstrated by the markedly increased *in vitro* osteogenic differentiation of MC3T3-E1 cells as well as by the enhanced regeneration of the critical-sized calvarial defects *in vivo*. We also showed that delayed L51P stimulation produced a significant increase in the BMP2-induced osteogenic differentiation of MC3T3-E1 cells and the luciferase activity in C2C12 cells. Moreover, we demonstrated for the first time that simultaneous and delayed L51P stimulation play an important role in the affinity of BMP2 cell binding.

It is well known that the high doses of BMPs required to induce sufficient bone healing in large mammals and humans are expensive and may produce negative side effects [28]. Milligram doses of BMPs are needed to induce sufficient bone repair, whereas only nanogram doses of BMPs are normally present in the human body. BMPs may be used in an efficient fashion if the price of BMPs is reduced or if the total required dose of BMPs is decreased [29]. As a result, there is an urgent need to modulate the strategies used to enhance the inductive capability of bone through BMP administration along

with the negative feedback regulation of BMP inhibitor [30]. Many earlier studies have attempted to develop a proper matrix to ensure the delivery of growth factors to the implantation site. Although matrix design is important to produce the proper concentration of BMPs at the implantation site [31], a novel approach to target BMP antagonists has been suggested [17].

Previous studies have not only identified Id1 as an early response gene that is induced by BMP2 in various types of mouse and human cells [32] but have also shown the effects of BMPs on the expression of Ids requires BMP/SMAD signaling [33]. Moreover, BMP antagonists have several important functions, such that osteogenesis is ultimately controlled by a fine balance between the levels of BMPs and their antagonists [34]. An earlier study by Christoph E. Albers and colleagues demonstrated that Noggin inhibited the BMP2-induced SMAD signaling, although L51P neutralize the Noggin-mediated inhibition, it is still unclear whether L51P can regulate the BMP2-induced negative feedback under the natural biological condition. We observed that BMP2 and BMP2/L51P combination groups showed equal activation of p-SMAD-1/5/8 even after 48 hours of stimulation. In contrast, delayed addition of L51P

to previously stimulated BMP2 cells significantly enhanced the expression of p-SMAD-1/5/8.

Based on our observation that the expression levels of BMP2 antagonists are significantly upregulated 1 and 3 days after BMP2 stimulation, we hypothesized that the application of L51P at a time after BMP2 stimulation might be more effective. It was important to use a conditioned medium to mimic the natural effect of BMP antagonists by using a protein binding assay. An analysis in such simulated medium can provide precise information about the cell binding behavior of BMP2 in the presence of L51P in a simultaneous and delayed manner. Our results are exciting for several reasons. First, we have documented the significance of BMP antagonists in hindering the cell binding affinity of BMP2. Second, we have directly confirmed the importance of the addition of L51P to BMP2 to enhance its cell binding capability. Finally, these results highlight the importance of timing in targeting these antagonists. This result would help to explain the increased efficiency of p-SMAD-1/5/8 with delayed L51P stimulation. The effects of BMP2 on osteoblastic differentiation and bone-specific gene expression levels are well known [35, 36]. We showed that the delayed addition of L51P to BMP2 increase

the gene expression levels of early osteogenic markers, *Alp* and *Osx*, relative to cultures stimulated simultaneously with BMP2 and L51P (Table 3). In addition, it produced a noticeable increase in ALP staining after 3 days compared to 7 days after the simultaneous addition of L51P and BMP2. From our *in vitro* results, we could confirm that delayed stimulation with L51P can down regulate the negative feedback that is normally placed on BMP activity.

In this study, we first confirmed that subcutaneously implanted BMP2/L51P-adsorbed exhibited enhanced osteogenic potential compared with BMP2-adsorbed hydrogels. Hans-Jörg Sebald and colleagues recently used L51P/BMP2 combination to induce bone regeneration through ceramic β-tricalcium phosphate carriers [19]. Approximately 60 % of the total protein amount was released from the carrier within 24 hours. Here, we used a gelatin hydrogel, which has previously been found to be a good carrier for the long-term delivery of growth factors. We showed that the continuous release of BMP2/L51P *in vivo* over 4 weeks induced a higher degree of bone formation than BMP2. This suggests that using a carrier enabling a prolonged retention L51P together with short retention BMP2 carrier may develop a delayed L51P *in vivo* environment. It

would therefore be interesting to develop such an *in vivo* system to assess the potential therapeutic value of this approach. We also believe that changing the water content of the gelatin hydrogel used in this study could produce a delayed protein-releasing pattern in both BMP2 and L51P [37].

A schematic model was proposed to summarize our findings (Fig. 10). BMP signals can be blocked by extracellular antagonists that bind BMP ligands and prevent their association with the BMP receptor (Fig. 10A). L51P specifically binds to BMP antagonists, allowing BMP signaling to proceed to osteoinduction (Fig. 10B). The timing of the targeting of BMP2 antagonists is crucial. The delayed addition of L51P was important to diminish the levels of free BMP antagonists in the extracellular space, encouraging receptor activation by BMPs and significantly strengthening the signaling pathway (Fig. 10C).

In summary, our study provides important evidence to support the positive function of L51P on BMP2 during bone regeneration. In fact, this combination significantly enhanced BMP2-induced osteoblastic differentiation. In contrast, L51P alone was not sufficient to induce any osteogenic potential. Our data demonstrated for the first time

the value of delayed L51P administration, which might provide a new research avenue for the cooperation between BMP2 and L51P. It is possible that these data may help eliminate the use of high-concentration BMPs, diminishing their high costs and reducing their negative side effects while allowing for novel, non-invasive bone tissue engineering therapeutics.

Acknowledgments

The author thank Dr. Takuo Kuboki (Graduate School of Medicine, Dentistry and Pharmaceutical Sciences, Okayama University), Dr. Walter Sebald (Physiological Chemistry Department, Würzburg University, Germany), Dr. Mitsuaki Ono, Dr. S. Kubota and Dr. T. Hattori (Graduate School of Medicine, Dentistry and Pharmaceutical Sciences, Okayama University) for their kind help and useful suggestions. This study was supported by a Grant-in-Aid for Scientific Research (for K.N., No. 23890123) from the Ministry of Education, Science, Sports and Culture of Japan.

References

[1].Kloen P., Lauzier D., and Hamdy R.C. :Co-expression of BMPs and BMP-inhibitors in human fractures and non-unions. *Bone*. 2012;**51**:59-68.

[2].Gruber R., Koch H., Doll B.A., Tegmeier F., Einhorn T.A., and Hollinger J.O. Fracture healing in elderly patient. *Exp. Gerontol*. 2006;**41**:1080-93.

[3].ParK J., Ries J., Gelse K., et al. Bone regeneration in critical size defects by cell-mediated BMP-2 gene transfer: a comparison of adenoviral vectors and liposomes. *Gene Ther*. 2003;**10**:1089-98.

[4].Mizrahi O., Sheyn D., Tawackoli W., et al. BMP-6 is more efficient in bone formation than BMP-2 when overexpressed in mesenchymal stem cells. *Gene Ther.* 2013;**20**:370-7.

[5].Gautschi O.P., Frey S.P., Zwellweger R. Bone morphogenetic proteins in clinical applications. *ANZ. J. Surg*. 2007;**77**:626-31.

[6].Wozney M. Overview of bone morphogenetic proteins. *Spine* 2002;**27** Suppl 1:S2-8.

[7].Egermann M., Lill C.A., Griesbeck K., et al. Effect of BMP-2 gene transfer on bone healing in sheep. *Gene Ther.* 2006;**13**:1290-9.

[8].Friendlaender G.E., Perry C.R., Cole J.D., et al. Osteogenic protein-1 (bone

morphogenetic protein-7) in the treatment of tibial nonunions. *J. Bone Joint Surg. Am.* 2001;**83** Suppl 1:S151-8.

[9].Govender S., Csimma C., Genant H.K., et al. Recombinant human bone morphogenetic protein-2 for treatment of open tibial fractures: a prospective, controlled, randomized study of four hudred and fifty patients. *J. Bone Joint Surg. Am*. 2002;**84**:2123-34.

[10].Morz T.E., Wang J.C., Hashinoto R., and Norvell D.C. Complications related to osteobiologics use in spine surgery: a systemic review. *Spine* 2010;**35** Suppl 9:S86-104.

[11].Estrada K.D., Retting K.N., Chin A.M., and Lyons K.M. Smad6 is essential to limit BMP signaling during cartilage development. *J. Bone Miner. Res.* 2011;**26**:2498-510.

[12].Wrana JL. Structural biology: On the wings of inhibition. *Nature.* 2002;420:613-4.

[13].Wan D.C., Pomerantz J.H., Brunet L.J., et al. Noggin suppression enhances in vitro osteogenesis and accelerates in vivo bone formation. J Biol Chem. 2007;**282**:26450-9.

[14].Mikawa S, Sato K. Chordin expression in the adult rat brain. *Neuroscience.* 2013;258:16-33.

[15].Fajardo M., Liu C.J., and Egol K. Levels of expressions for BMP-7 and several

BMP antagonists may play an integral role in a fracture nonunion: a pilot study. *Clin. Orthop. Relat. Res.* 2009;**467**:3071-8

[16].Montjovent M.O., Siegrist M., Klenke F., Wetterwald A., Dolder S., and Hofstetter W. Expression of antagonists of WNT and BMP signaling after non-rigid fixation of ostoetomies. *Bone.* 2013;**53**:79-86.

[17].Keller S., Nickel J., Zhang J.L., Sebald W., and Mueller T.D. Molecular recognition of BMP-2 and BMP receptor IA. *Nat. Struct. Mol. Biol.* 2004;**11**:481-8.

[18].Albers C.E., Hofstetter W., Sebald H.J., Sebald W., Siebenrock K.A., and Klenke F.M. L51P – A BMP2 variant with osteoinductive activity via inhibition of Noggin. *Bone*. 2012;**5**:401-6.

[19].Sebald H.J., Klenke F.M., Siegrist M., Albers C.E., Sebald W., and Hofstetter W. Inhibition of endogenous antagonists with an engineered BMP-2 variant increases BMP-2 efficacy in rat femoral defect healing. *Acta Biomater*. 2012;**8**:3816-20.

[20].Zilberg L., ten Dijke O., Sakai L.Y., and Rifkin D.B. A rapid and sensitive bioassay to measure bone morphogenetic protein activity. *BMC Cell Biol.* 2007;**8**:41.

[21].Yamamoto M., Tabata Y., Ikada Y. Ectopic bone formation induced by

biodegradable hydrogels incorporating bone morphogenetic protein. *J. Biomater. Sci. Polym. Ed*. 1998;**9**:439-58.

[22].Nakamura Y., Wakitani S., Nakayama J., Wakabayashi S., Horiuchi H., and Takaoka K. Temporal and spatial expression profiles of BMP receptors and noggin during BMP-2 induced ectopic bone formation. *J. Bone Miner. Res.* 2003;**18**:1854-62.

[23].Gao X., Usas A., Lu A., et al. BMP2 is superior to BMP4 for promoting human muscle derived-stem cell mediated bone regeneration in critical size calvarial defect model. *Cell Transplant.* 2013;**22**:2393-408.

[24].Levi B., James A.W., Nelson E.R., et al. Human adipose derived stromal cells heal critical size mouse calvarial defects. *PLoS One.* 2010;**5**:e11177.

[25].Komatsu Y., Yu P.B., Kamiya N., et al. Augmentation of Smad-dependent BMP signaling in neural crest cells causes craniocynostosis in mice. *J. Bone Miner. Res*. 2013;**28**:1422-33.

[26].Chen X.D., Fisher L.W., Robey P.G., and Young M.F. The small leucine-rich proteoglycan biglycan modulates BMP-4-induced osteoblast differentiation. *FASEB J*. 2004;**18**;948-58.

[27].Nagata M., Hoshina H., Li M., et al. A clinical study of alveolar bone tissue engineering with cultured autogenous periosteal cells: coordinated activation of bone formation and resorption. *Bone.* 2012;**50**:1123-9.

[28].Zara JN, Siu RK, Zhang X, et al. High doses of bone morphogenetic protein 2 induce structurally bone and inflammation in vivo. *Tissue Eng. Part A.* 2011;**17**:1389-99.

[29].Garrison K.R., Donell S., Ryder J., et al. Clinical effectiveness and cost-effectiveness of bone morphogenetic protein in the non-healing of fracture and spinal fusion: a systemic review. *Health Technol. Assess.* 2007;**11**:1-150,iii-iv.

[30].Tsialogiannis E., Polyzois I., Oak Tang Q., et al. Targeting bone morphogenetic protein antagonists: in vitro and in vivo evidence of their role in bone metabolism. *Expert Opin. Ther. Taregts.* 2009;**13**:123-37.

[31].Sykaras N., and Opperman L.A. Bone morphogenetic proteins (BMPs): how do they function and what can they offer for the clinician? *J. Oral Sci.* 2003;**45**:57-73.

[32].Clement J.H., Marr N., Meissner A.. Bone morphogenetic protein 2 (BMP-2) induces sequential changes of Id gene expression in the breast cancer cell line MCF-7. *J.*

Cancer Res. Clin. Oncol. 2000;**126**:271-9.

[33].Langenfeld E.M., Kong Y., and Langenfeld J. Bone morphogenetic protein 2 stimulation of tumor growth involves the activation of Smad-1/5. *Oncogene.* 2006;**25**:685-92.

[34].Ono M., Inkoson C.A., Kilts T.M., and Young M.F. WISP-1/CCN4 regulates osteogenesis by enhancing BMP-2 activity. *J. Bone Miner. Res.* 2011;**26**:193-208.

[35].Yang Q., Jian J., Abramson S.B., Huang X. Inhibitory effects of iron on bone morphogenetic 2-induced osteoblastogenesis. *J. Bone Miner. Res*. 2011;**26**:1188-96.

[36].Skillington J., Choy L., and Derynck R. Bone morphogenetic protein and retinoic acid signaling cooperate to induce osteoblasts differentiation or preadipocytes. *J. Cell Biol.* 2002;**159**:135-46.

[37].Yamamoto M., Takahashi Y., and Tabata Y. Controlled release by biodegradable hydrogels enhances the ectopic bone formation of bone morphogenetic protein. *Biomaterials.* 2003;**24**:4375-83.

Figure Legends

Fig. 1. The effect of the simultaneous addition of L51P to BMP2 on osteogenic differentiation

(A) MC3T3-E1 cells were stimulated with BMP2 and/or L51P for the indicated duration, and the levels of p-SMAD-1/5/8 and total-SMAD-1 were detected by western blot. β-ACTIN served as an internal control. (B) To test the BMP-sensitive Id1 promoter activation, C2C12 cells were stimulated with BMP2 and/or L51P for 24 hours, and the luciferase activity was measured. (C, D) Relative mRNA expression levels of *Alp* (C) and *Osx* (D) were measured by real-time RT-PCR 1 or 3 days after stimulation with BMP2 and/or L51P. The expression of each gene was normalized relative to *S29* ribosomal protein RNA. Data are reported as the mean ± SE (n=3). {** $p < 0.01$, *** $p < 0.001$ versus the non-stimulation group, ## $p < 0.01$, ### $p < 0.001$ versus the BMP2 stimulation group (one-way ANOVA/Tukey)}. Data are representative of at least three different experiments.

Fig. 2. Gene expression patterns of BMP antagonists in MC3T3-E1 cells after BMP2 stimulation

MC3T3-E1 cells were cultured with 100 ng/mL BMP2, and total RNA was collected at 0, 1, 3, 5, and 7 days. The mRNA expression levels of *Nog* (A), *Grem 1* (B) and *Chord* (C) were subsequently evaluated by real-time RT-PCR. The expression of each gene was normalized relative to *S29* ribosomal RNA. Data are reported as the mean ± SE (n=3). {*** $p < 0.001$ versus the non-stimulated group (two-way ANOVA/Tukey)}. Data are representative of at least three different experiments.

Fig. 3. The effect of delayed L51P stimulation on BMP2-induced osteogenic differentiation

A schematic of the delayed L51P stimulation experiment is shown in (A). (B) To test the effect of the delayed addition of L51P, MC3T3-E1 cells and C2C12-BRE-Luc cells were stimulated by L51P after 3 days of BMP2 induction. After 15 min of L51P stimulation, the total cell lysates were collected, and p-SMAD-1/5/8 and total-SMAD-1 were detected by western blot. β-ACTIN served as an internal control. (C) To analyze the activity of the BMP-sensitive Id1 promoter, the cell lysate of the C2C12-BRE-Luc cells was collected 24 hours after stimulation, and a luciferase assay was performed.

Data are reported as the mean ± SE (n=6). (D, F) Total RNA was collected at 1 and 7 days after L51P stimulation, and the mRNA expression levels of *Alp* and *Osx* were evaluated by real-time RT-PCR. The expression of each gene was normalized relative to *S29* ribosomal protein RNA. Data are reported as the mean ± SE (n=3). (E) ALP staining assay after 3 days. {** $p < 0.01$, *** $p < 0.001$ versus non-stimulation group, ### $p < 0.001$ versus BMP2 stimulation group (One-way ANOVA/Tukey)}. Data are representative of two different experiments.

Fig. 4. The affinity of BMP2 to MC3T3-E1 cells with L51P stimulation

(A, B) To evaluate whether L51P regulates BMP2 binding to the cell, fixed cells were treated with BMP2 (500 ng/mL) and/or L51P (500, 1000 ng/mL) in conditioned medium (0.1 % basal medium collected from cells stimulated with 500 ng/mL BMP2 for 3 days) for 4 hours. After incubation, BMP2 positive cells were detected by measuring immunoreactivity toward the anti-BMP2 antibody. The graph shows the quantification of these data. Data are reported as the mean ± SE (n=3). {*** $p < 0.001$ versus non-stimulation group, ## $p < 0.01$, ### $p < 0.001$ versus BMP2 group incubated

in conditioned medium only (black column) (One-way ANOVA/Tukey)}. Data are representative of two different experiments.

Fig. 5. The effect of the BMP2/L51P combination on osteogenic differentiation under long-term culture conditions

(A) MC3T3-E1 cells were cultured with BMP2 and/or L51P in osteogenic differentiation medium. ALP and Alizarin red S staining were performed 1 and 4 weeks after stimulation, respectively. (B) Quantitative evaluation of Alizarin red S staining. Data are reported as the mean ± SE (n=3). (C) Total RNA was collected at 3 weeks after stimulation, and the mRNA expression levels of *Ocn* were evaluated by real-time RT-PCR. The expression of each gene was normalized relative to *S29* ribosomal protein RNA. Data are reported as the mean ± SE (n=3). {* $p < 0.05$, *** $p < 0.001$ versus non-stimulation group, # $p < 0.05$, ## $p < 0.01$, ### $p < 0.001$ versus BMP2 stimulation group (one-way ANOVA/Tukey)}. Data are representative of at least three different experiments.

Fig. 6. Photographic image (A-D), radiographic image (E-H) and histological section (I-P) of ectopic bone tissues 2 weeks after implantation of hydrogel with BMP2 (10 μg) and/or L51P (10 μg)

(A-H) Arrows indicate the newly formed bone, and asterisks indicate the residual hydrogel. (I-P) HE staining of histological sections of ectopic formed bone. Arrows, arrowheads and asterisks indicate the newly formed bone, the fibrosis tissue and the residual hydrogel, respectively. (M, N) High-magnification views of K (O, P) High-magnification views of L.

Fig. 7. Three-dimensional micro-CT images of the rat calvarial bone defects at 4 weeks after surgery (A), and the mean normalized radio-opacity (NRO) of the defects against the peripheral original bone (B)

(A) Micro-CT images of rat calvaria show that the BMP2 and L51P combination induces bone formation more effectively than the L51P and BMP2 groups. (B) Quantification of the micro-CT images was performed using ImageJ software. Significant increases in bone healing were detected in the BMP2/L51P combination

group relative to the BMP2 group after 4 weeks of implantation. {** $p < 0.01$, *** $p < 0.001$: compared to control group, # $p < 0.05$, ## $p < 0.01$: compared to BMP2 group (One-way ANOVA/Tukey) }.

Fig. 8. The histological appearance of rat calvarial defects 4 weeks after implantation of the hydrogel with BMP2 and/or L51P

The calvarial defects in the BMP2/L51P (1 and 5 μg) combination groups (C, D) had more significant bone regeneration than those of the BMP2 group (F). In contrast, no obvious bone formation was observed in the no-hydrogel (B), hydrogel only (C), and L51P groups (D, E). (I), (J), and (K) show high-magnification views of (F), (G), and (H), respectively. Arrows, arrowheads and asterisks indicate the newly formed bone, the fibrous tissue and hydrogel, respectively.

Fig. 9. Higher magnification of immunohistological analysis and TRAP staining analysis of the rat calvarial defects at 4 weeks after implantation of the hydrogel with the BMP2/L51P combination group and the BMP2 group

(A-D) Immunohistochemical analysis of OCN. Arrows indicate the OCN-positive osteoblast cells lining the surface of bone. (B) and (D) show high-magnification views of (A) and (C), respectively. A stronger signal intensity was observed in cells lining the groups treated with the BMP2/L51P combination. (E-H) TRAP staining of rat calvarial defects. Arrowheads indicate the TRAP-positive osteoclasts. (F) and (H) show the high-magnification views of (E) and (G), respectively. The number of TRAP positive cells was markedly increased in the BMP2/L51P combination group. Images are representative of three different experiments.

Fig. 10. A schematic diagram showing BMP signaling and the possible action of L51P

BMP initially binds to type I and II receptors, which subsequently phosphorylate a member of the SMAD family that translocates to the nucleus and upregulates BMP early-response genes, leading to increased bone formation. (A) The effect of BMP antagonists on BMP signaling subsequently downregulates bone formation. (B) The inhibition of such antagonists by L51P may result in an unopposed synergy between

BMP ligands and their receptors, resulting in enhanced osteogenesis. (C) Delayed targeting of BMP antagonists may positively counteract the normal negative feedback action exerted on BMP2 ligands, contributing to a significant increase in the osteogenic potential of BMP2.

Figures

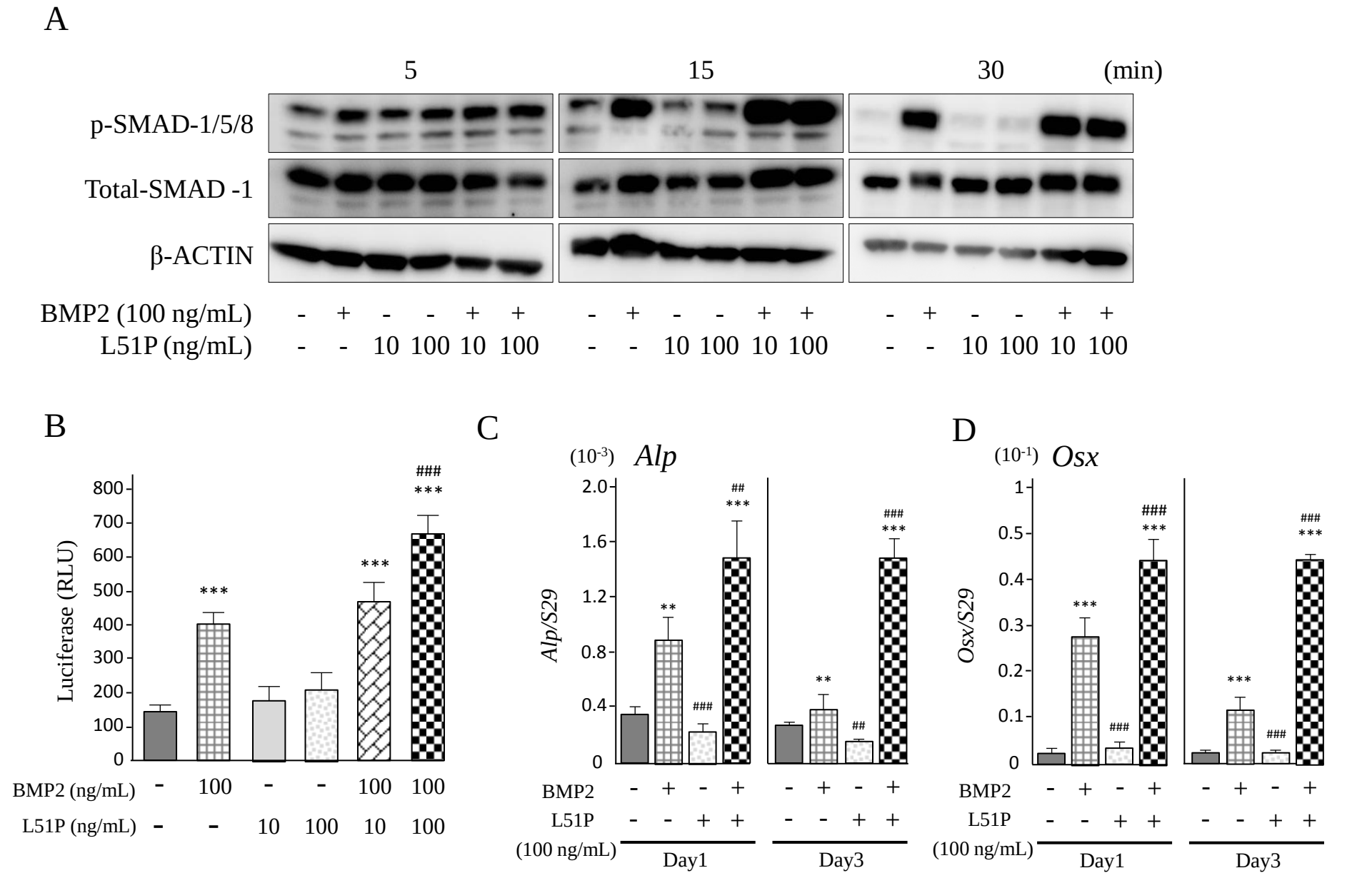

Figure 1 (Khattab et al.)

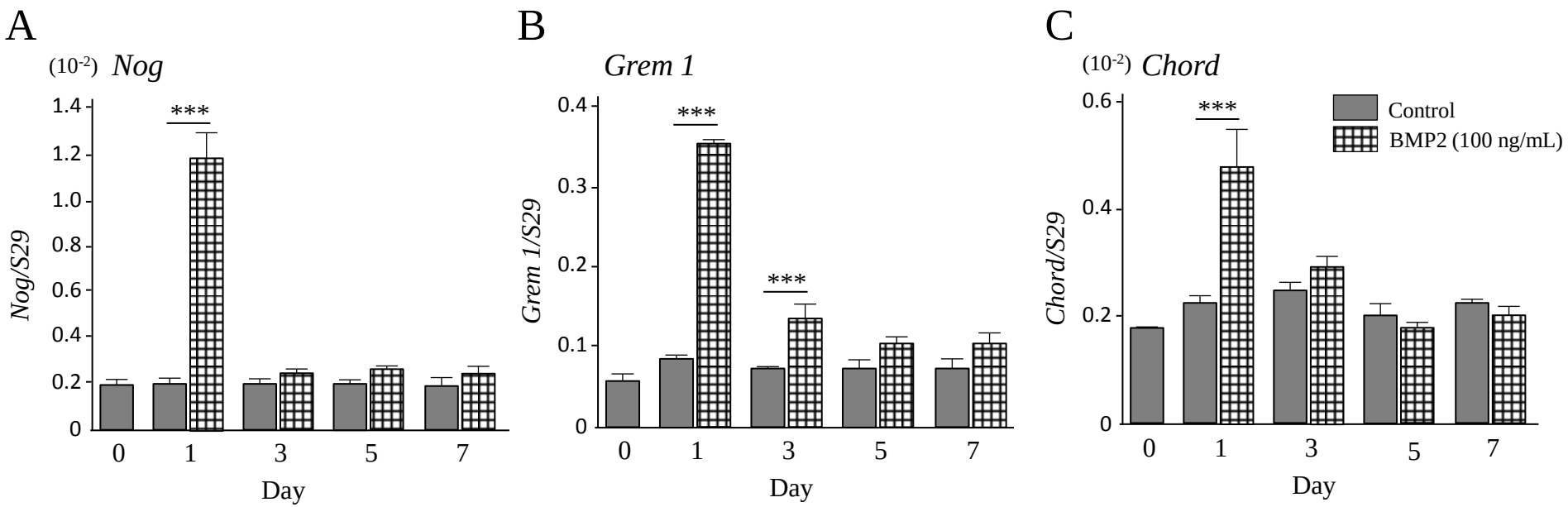

Figure 2 (Khattab et al.)

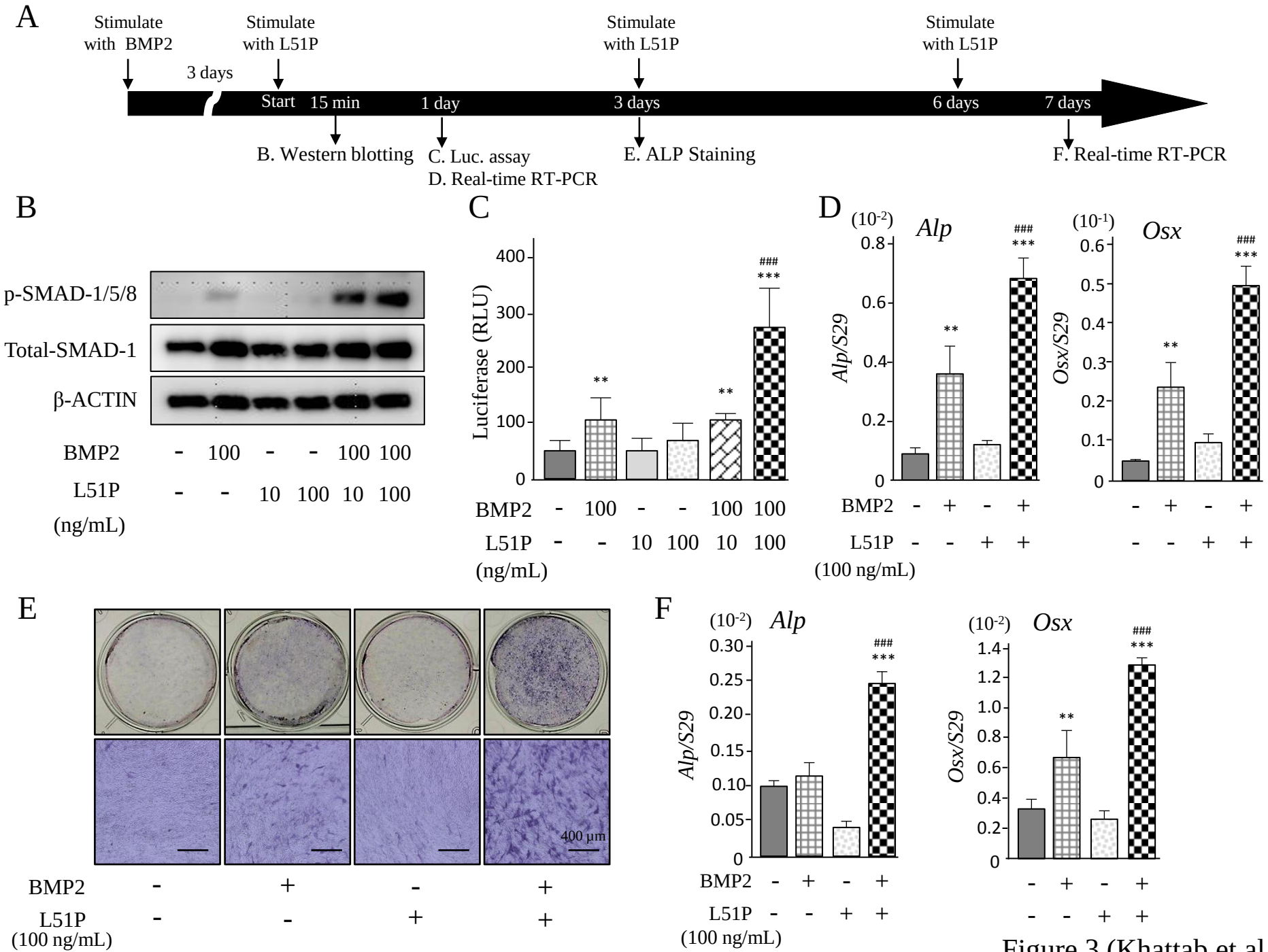

Figure 3 (Khattab et al.)

A

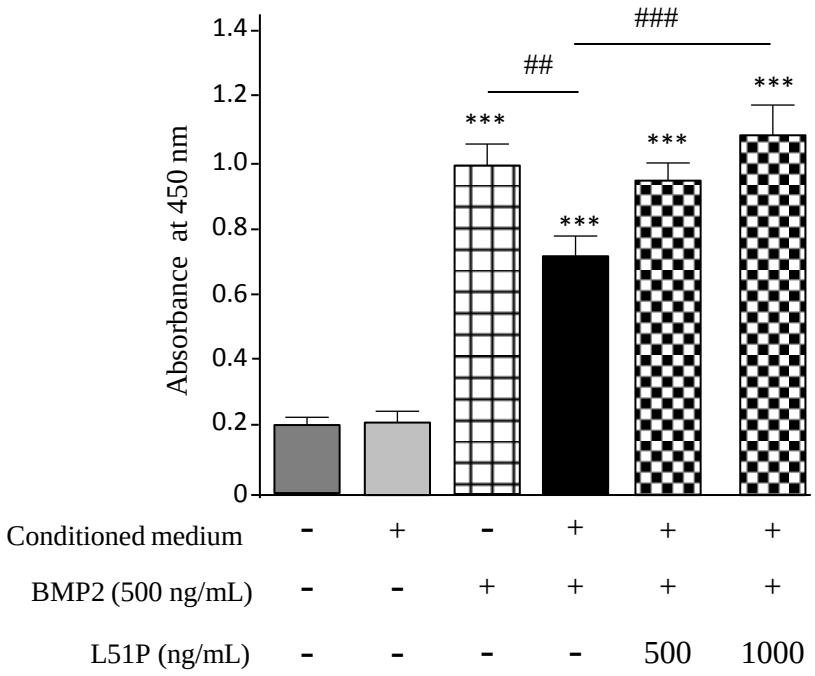

B

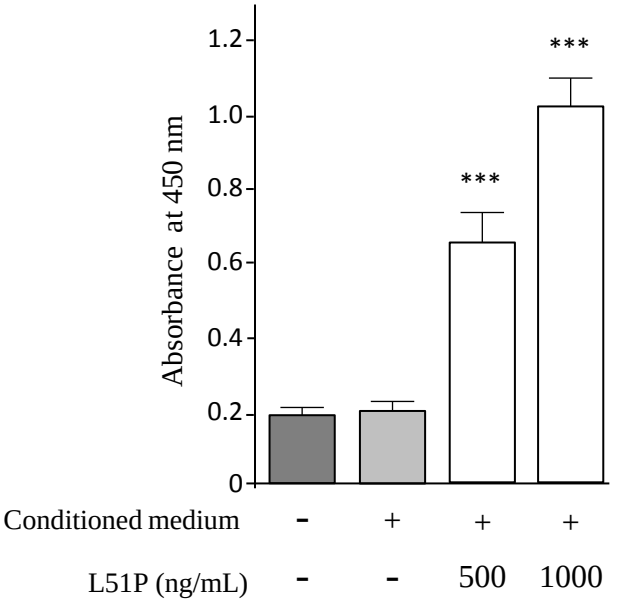

Figure 4 (Khattab et al.)

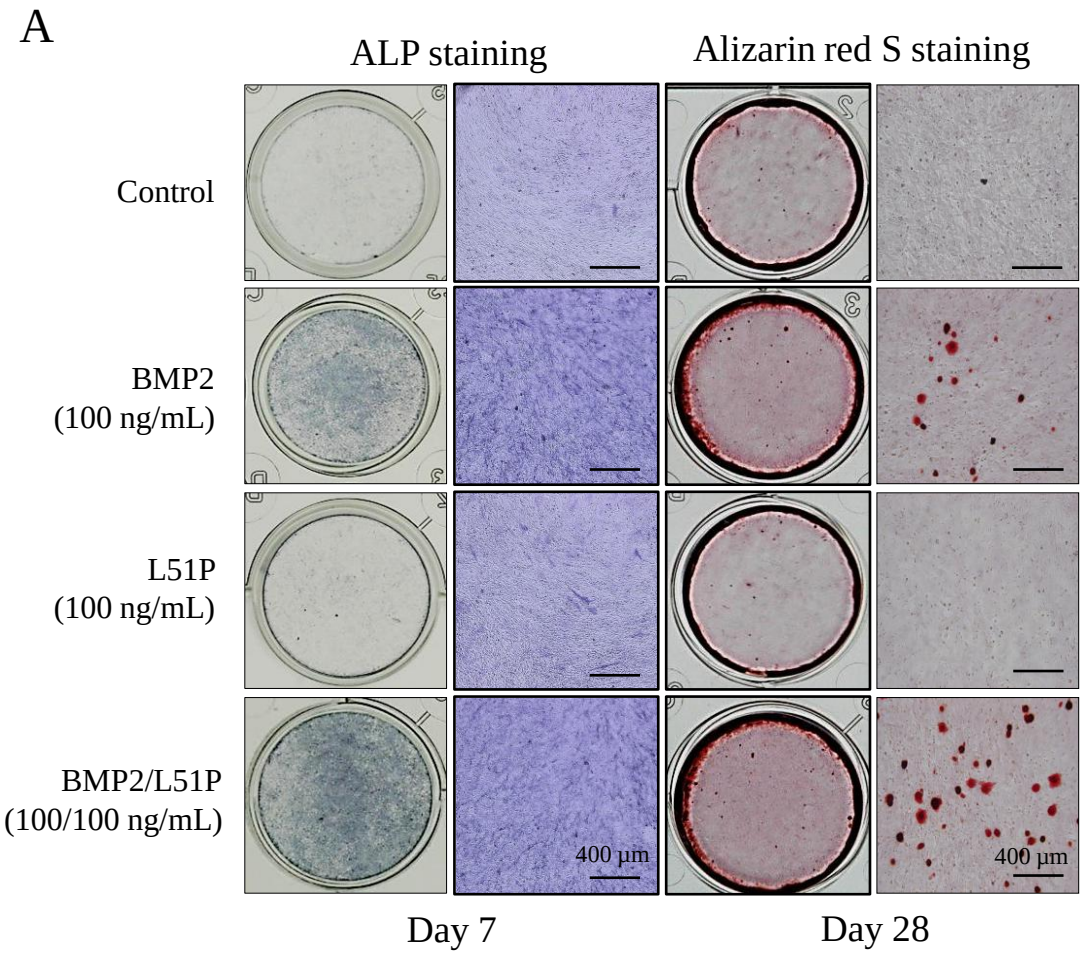

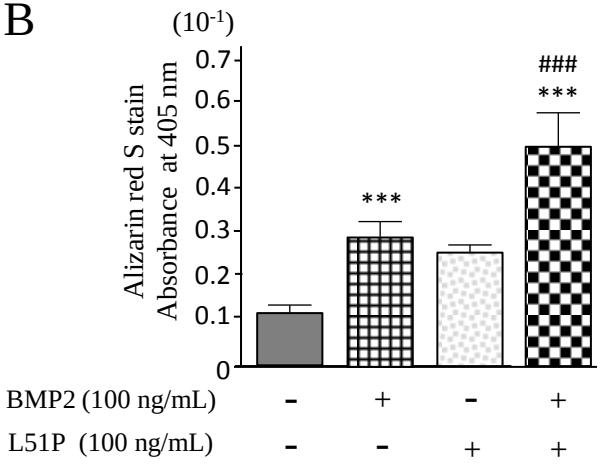

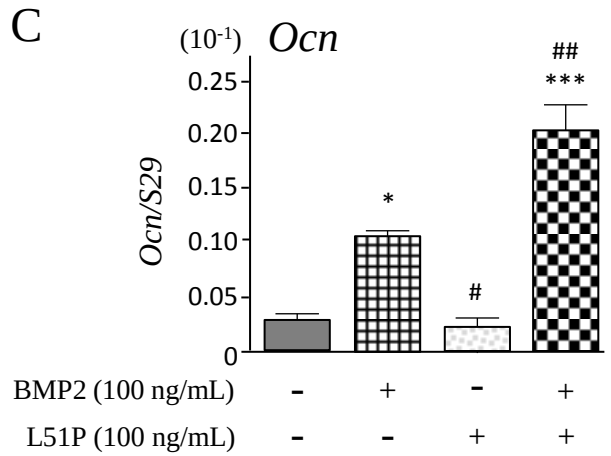

Figure 5 (Khattab et al.)

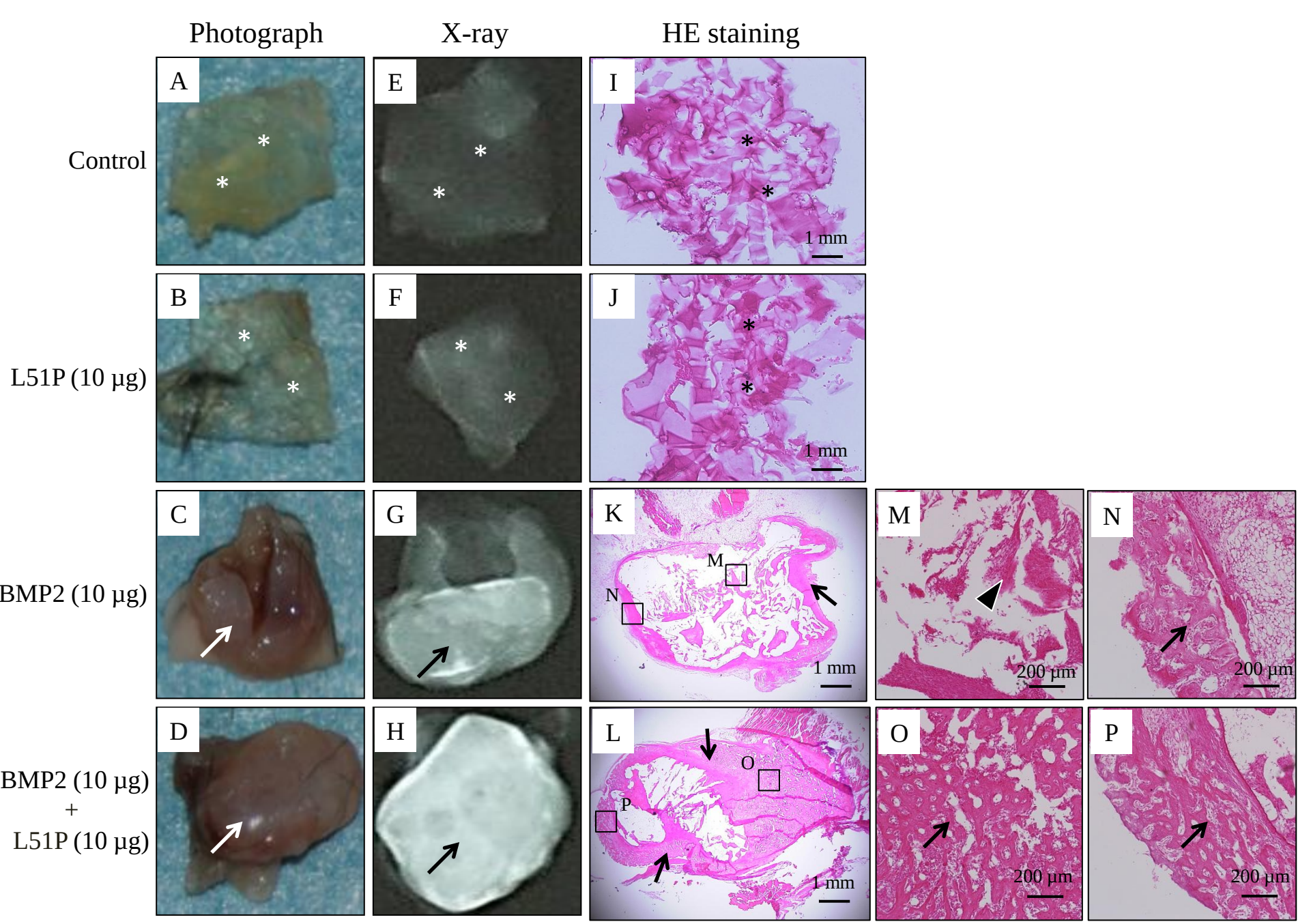

Figure 6 (Khattab et al.)

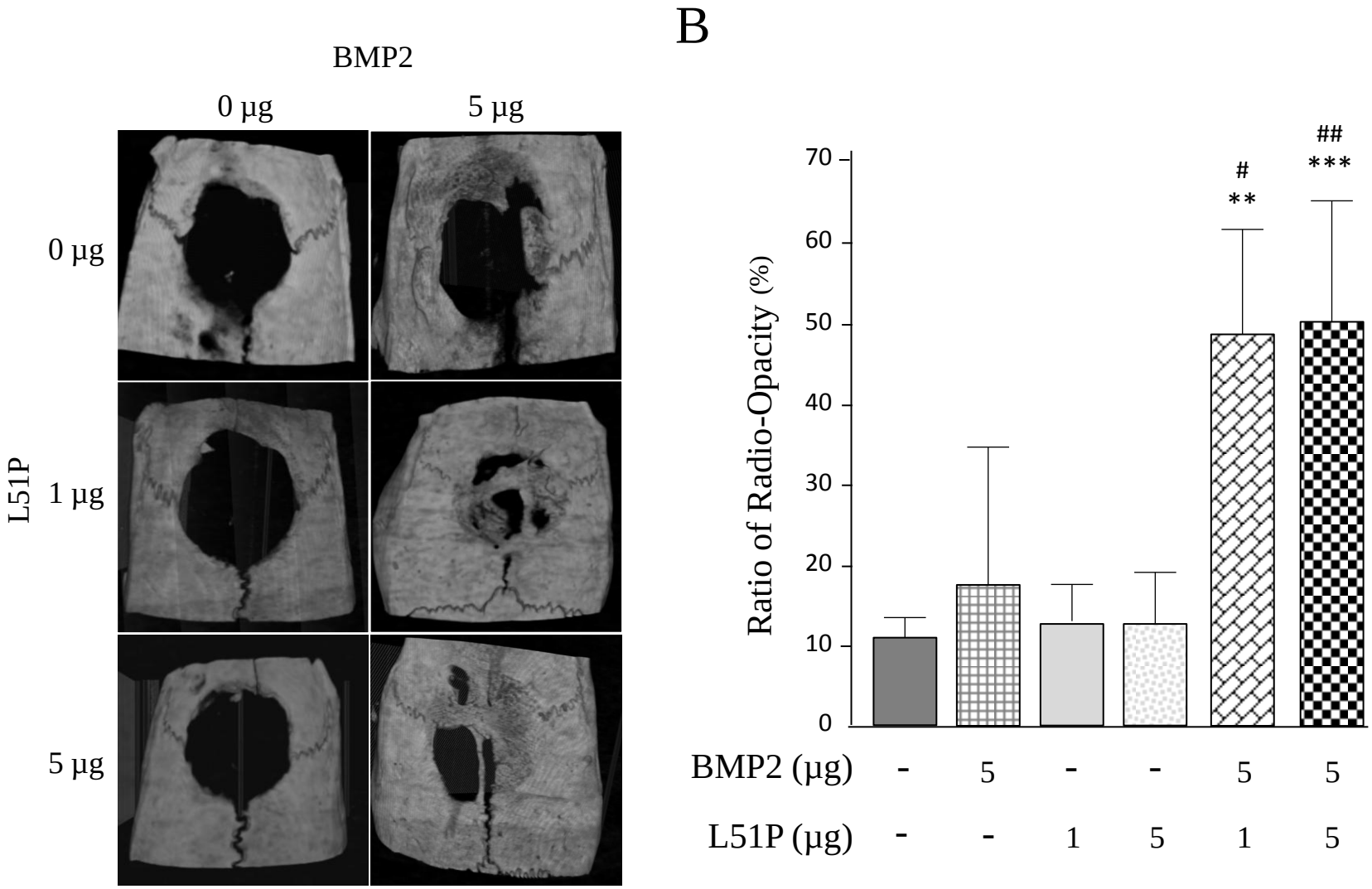

Figure 7 (Khattab et al.)

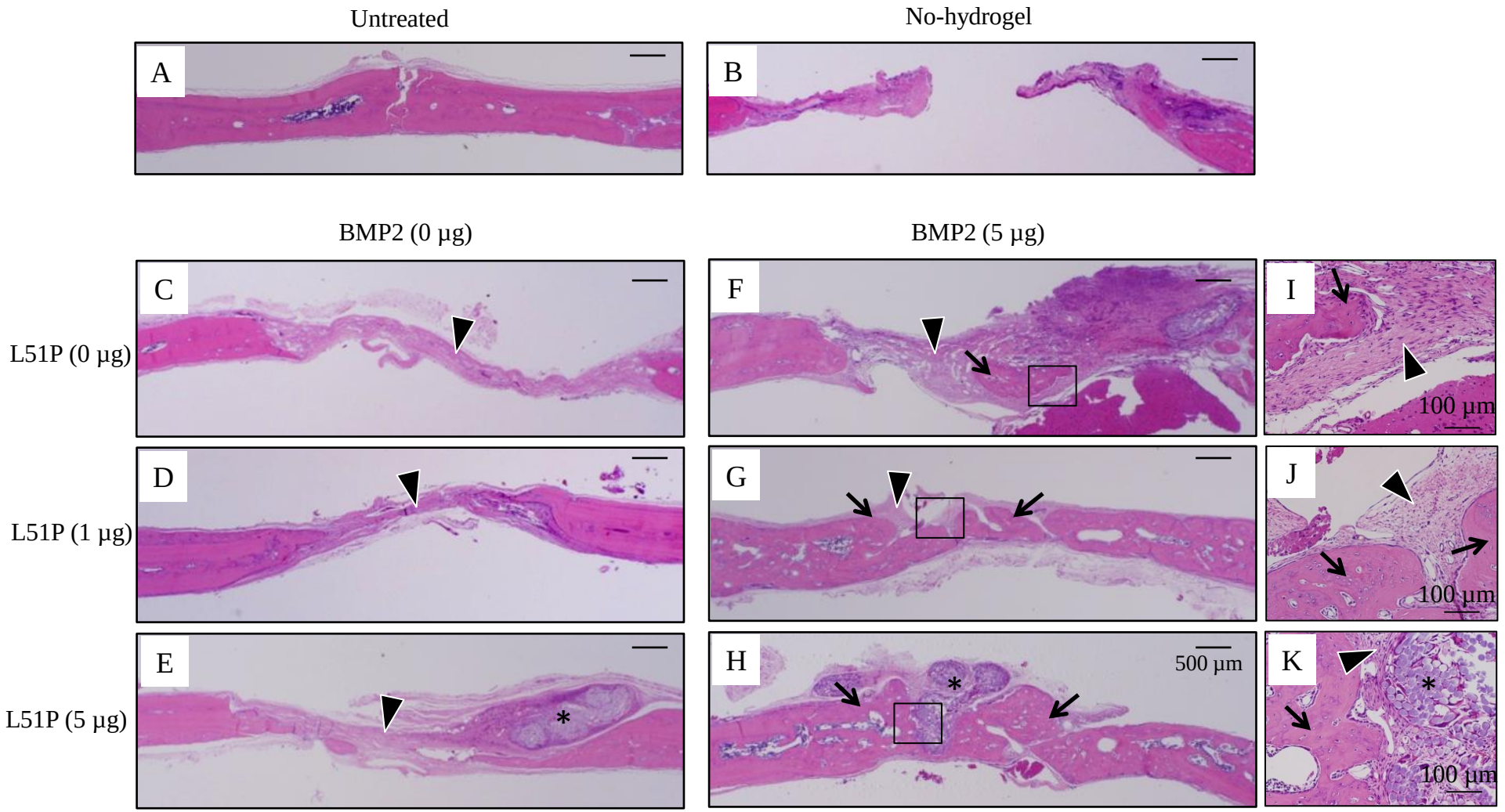

Figure 8 (Khattab et al.)

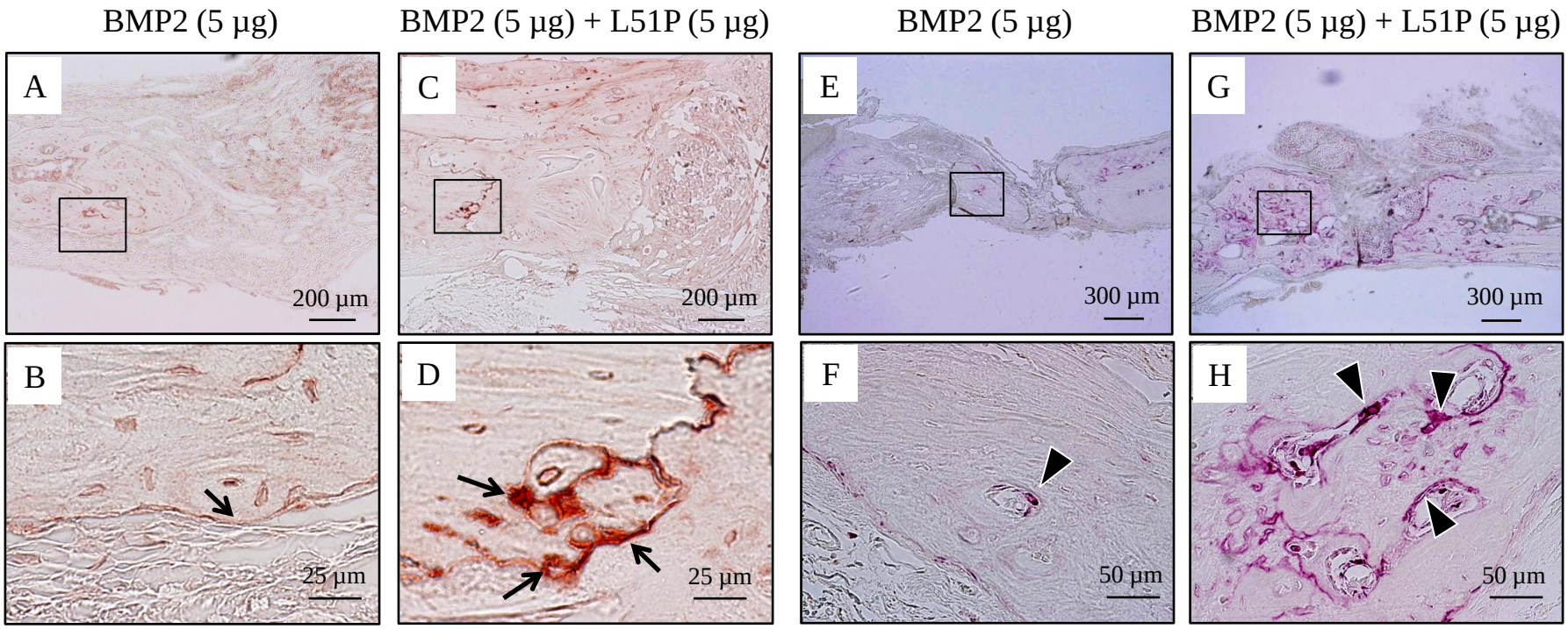

Figure 9 (Khattab et al.)

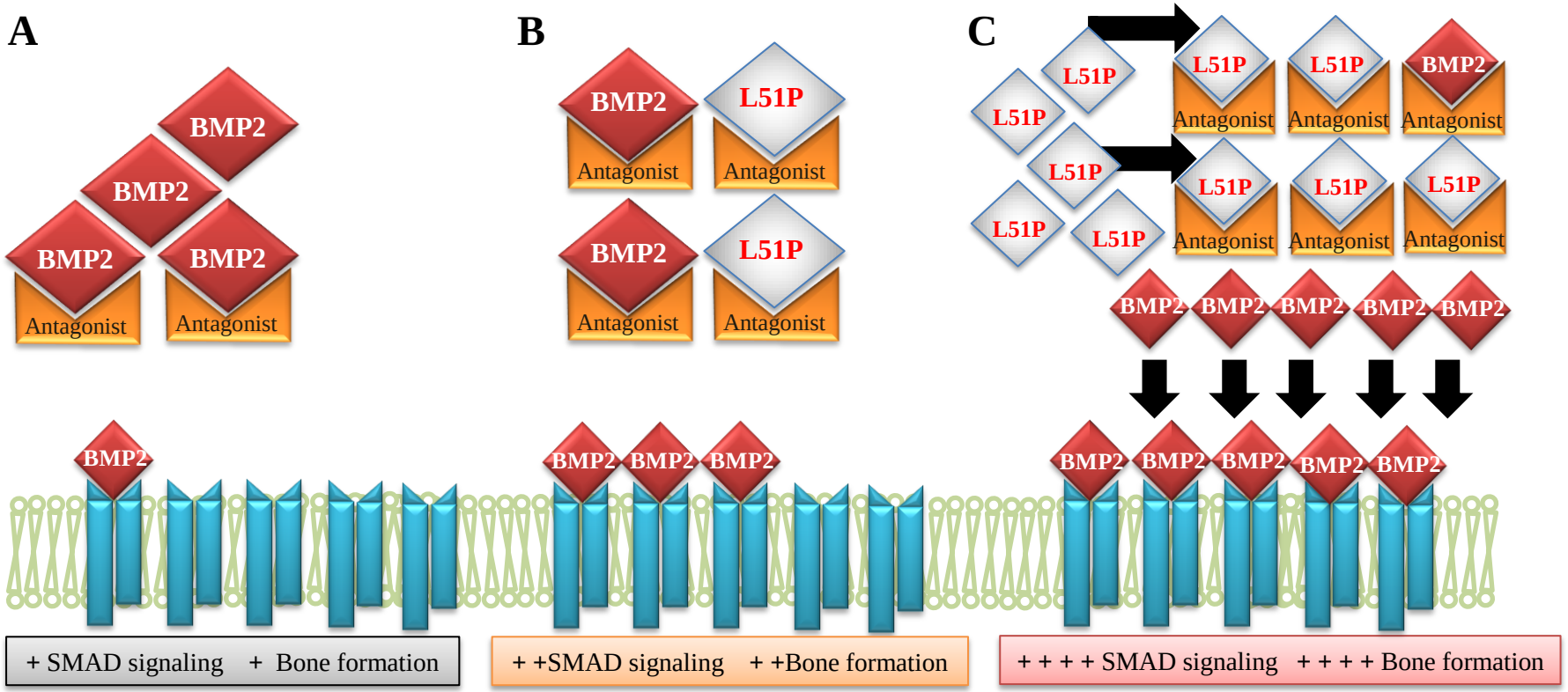

Figure 10 (Khattab et al.)

Tables

Table 1: Primers used for real-time RT-PCR analysis

Gene	*GenBank accession no.*	*Primer sequence*	*PCR product length (bp)*
S29	NM_009093	5`-TTCCTTTCTCCTCGTTGG-3` (S) 5`-ATGTTCAGCCCGTATTTG-3` (AS)	108
Alp	J02980	5`-SGCTCTCCCTACCGACCCTGTTC-3` (S) 5`-TGCTGGAAGTTGCCTGGACCTC-3` (AS)	130
Osx	BC113150	5`-ACGATGATGATGATGATGATGAT-3` (S) 5`-AACACCAATCTCCTTAACTCTG-3` (AS)	82
Nog	NM_008711	5`-CCACCTCCAACCAGTTTC-3` (S) 5`-AGGTCTCTGTAGCCAAGAA-3` (AS)	75
Grem1	NM_011824	5`-GAGAGGAGGTGCTTGAGT-3` (S) 5`-ATGATAGTGCGGCTGTTG-3` (AS)	133
Chord	AF069501	5`-AAGAGATGGACTGGTTGGA-3` (S) 5`-TGCCTGGTGGTGATGTAT-3` (AS)	97
Col I	NM_007742	5`-CTGGTCCTGCTGGTCCTGCTG-3` (S) 5`-TCTGTCACCTTGTTCGCCTGTCTC-3` (AS)	110
Ocn	BC055868	5`-CCAAGCAGGAGGGCAATAAGGTAG-3` (S) 5`-CTCGTCACAAGCAGGGTCAAGC-3` (AS)	122

S: sense, AS: antisense

Table 1 (Khattab et al.)

Table 2: Defects grouping

Group	*1*	*2*	*3*	*4*	*5*	*6*	*7*	*8*
	Untreated defect	*Control defect (No hydrogel)*	*Control defect (Hydrogel)*	*BMP2 (5 µg)*	*L51P (1 µg)*	*L51P (5 µg)*	*BMP2 (5 µg) + L51P (1 µg)*	*BMP2 (5 µg) + L51P (5 µg)*

Table 2 (Khattab et al.)

Table 3 : Fold change of mRNA expression levels normalized to BMP2

	Simultaneous L51P+BMP2	*Delayed L51P+BMP2*
Alp	*1.62*	*1.97*
Osx	*1.56*	*2.08*

Table 3 (Khattab et al.)